Characterizing the Transport Properties of Quasisymmetric Stellarators from Their Equivalent Tokamaks

Hongxuan Zhu[1], R. Gaur[2], Z. Lin[3], and A. Bhattacharjee[4]

[1]Zhejiang University, [2]University of Wisconsin, Madison, [3]University of California, Irvine, [4]Princeton University

The 16th International West Lake Symposium
April 10-12, 2026

Introduction: drift waves in tokamaks and stellarators

- Drift-wave turbulence are ubiquitous in tokamaks and stellarators.[1,2]
- They are highly anisotropic: $l_{\parallel} \gg l_{\perp}$, with $l_{\parallel} \sim R/\iota$ and $l_{\perp} \sim \rho_i$.
- The ion-temperature gradient (ITG) turbulence is known to limit the achievable ion temperature in electron-heated W7-X plasmas.[3]

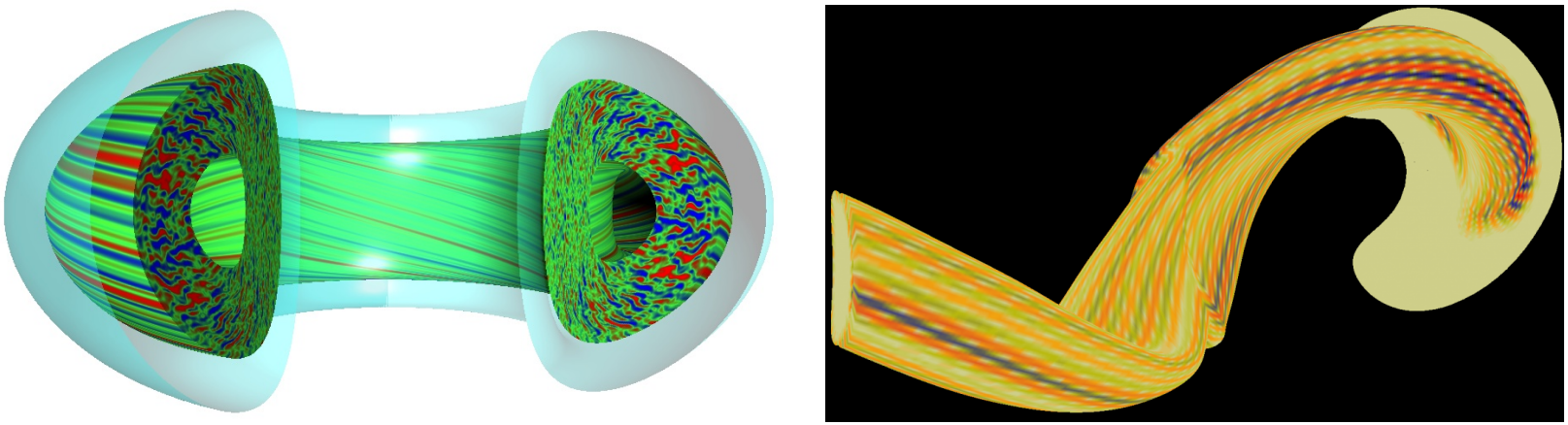

Figure 1: Microturbulence in tokamaks (left) and stellarators (right).

[1] https://w3.pppl.gov/~hammett/viz/viz.html
[2] https://sites.fusion.ciemat.es/multitranstell/turbulence/
[3] Beurskens *et al.*, Nucl. Fusion **61**, 116072 (2021).

Motivation: different stellarators show different level of ITG turbulent transport

From global GTC simulations, Chen *et al.* studied the ITG turbulence and zonal flows in several different stellarator configurations:[1]

- Gyrokinetic ions, adiabatic electrons.
- Ion temperature gradient $R/L_T \approx 6.9$, flat density profile.

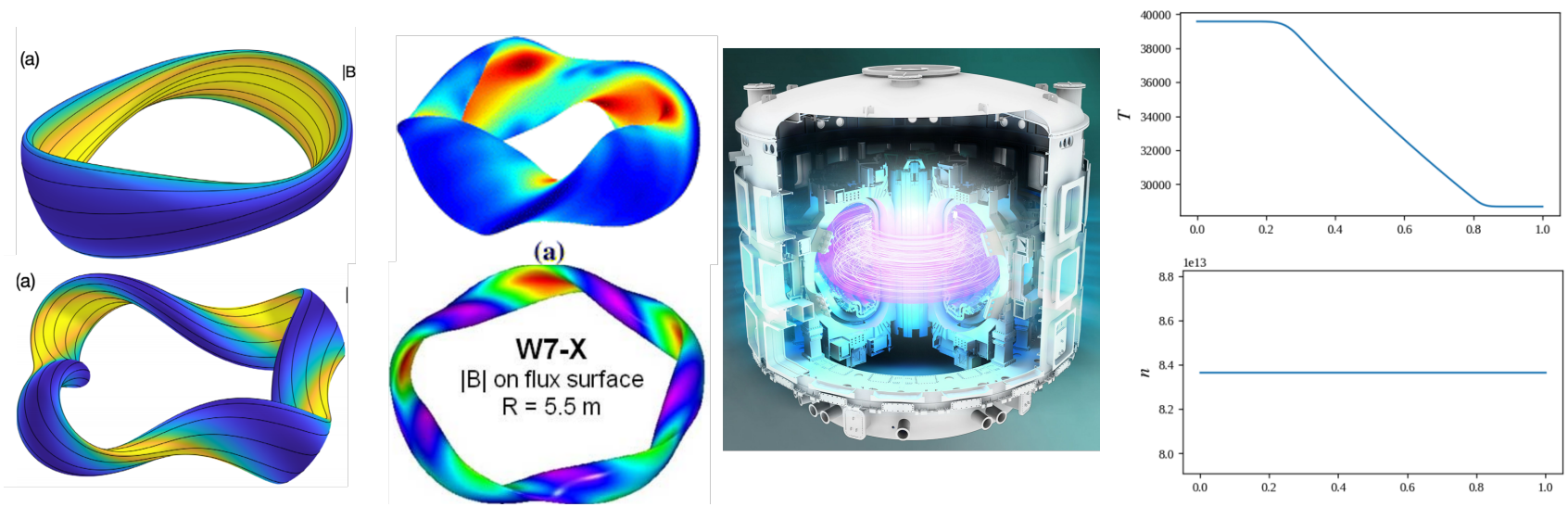

Figure 2: Quasi-axisymmetric (QA) and Quasi-helically symmetric (QH) configurations with self-consistent bootstrap currents[2]; NCSX; W7-X; ITER.

[1] H. Chen, X. Wei, H. Zhu, and Z. Lin, Nucl. Fusion **65**, 074002 (2025).

[2] M. Landreman, S. Buller, and M. Drevlak, Phys. Plasmas **29**, 082501 (2022).

Some terminology for stellarators

- To confine particles, the $|\boldsymbol{B}|$ contour must close in poloidal (P), helical (H), or toroidal (T/A) directions.
- Omnigenity: $\oint dl(\boldsymbol{v}_D \cdot \nabla\psi) = 0$ for trapped particles.
- Quasi-symmetry (QS): $|\boldsymbol{B}| = B(\psi, M\vartheta - N\zeta)$ in Boozer coordinates.
- W7-X is quasi-isodynamics (QI): OP but not QP.

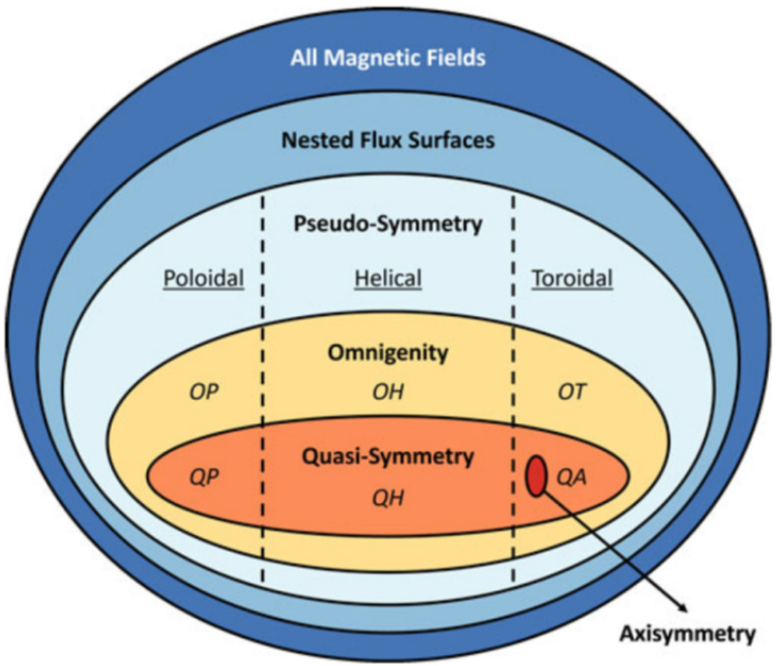

[1] Dudt *et al.* J. Plasma Phys. **90**, 905900120 (2024).

The QA configurations tend to exhibit much higher transport level compared to other configurations

At similar machine sizes and plasma parameters, the linear growth rate and nonlinear transport level show significantly different behaviors.[1]

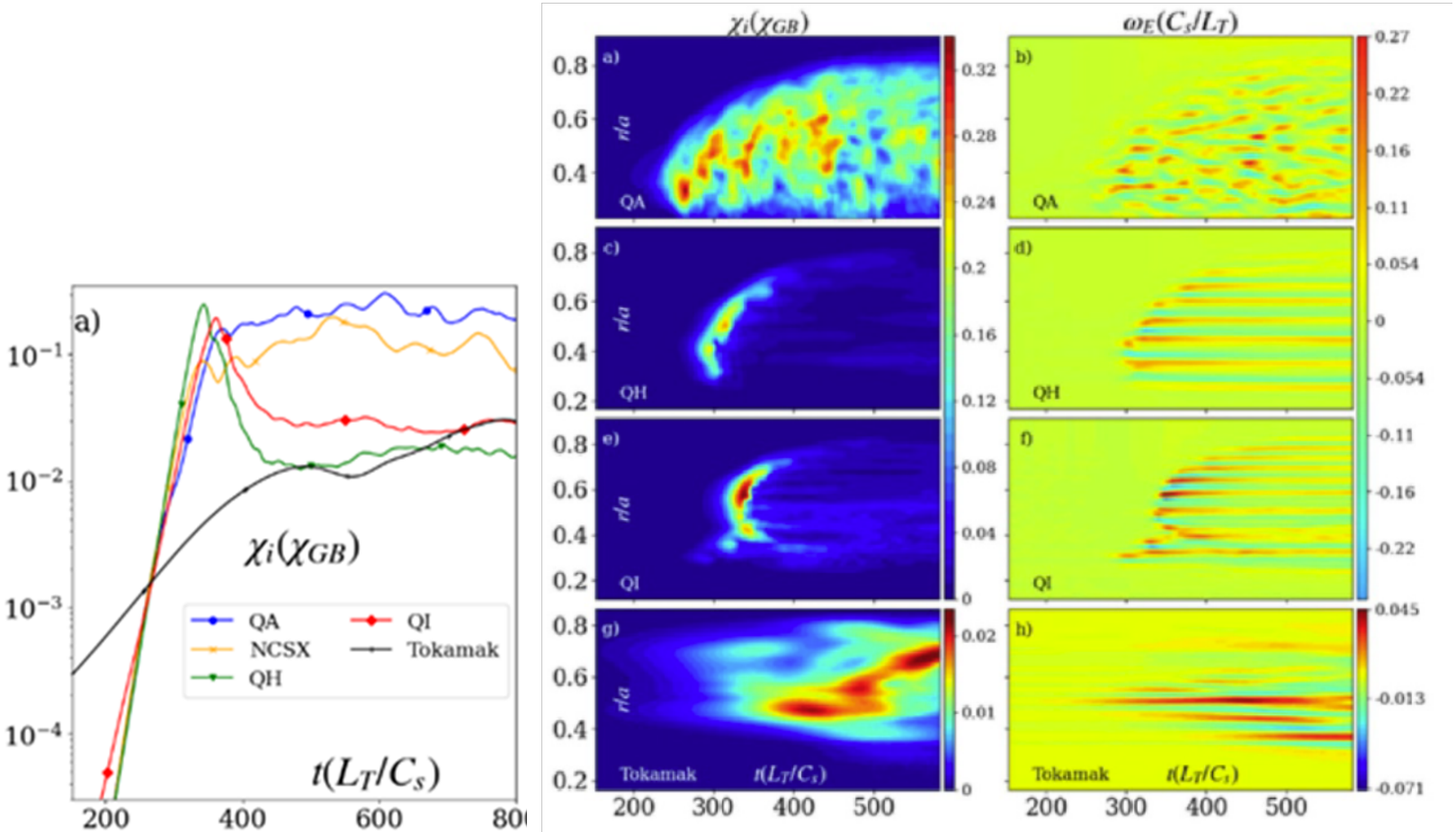

Figure 3: $\chi = Q/n|\nabla T|$: heat diffusivity (Q has the unit of $\mathrm{J/m^2 \cdot s}$); $\chi_{\mathrm{GB}} = \rho_s^2 C_s/L_T$: gyro-Bohm diffusivity; ω_E: zonal-flow shearing rate.

[1] H. Chen, X. Wei, H. Zhu, and Z. Lin, Nucl. Fusion **65**, 074002 (2025).

How do we understand the transport properties in different stellarator configurations?

The above study indicated that QA is at disadvantage regarding turbulent transport, but there are more questions to answer:

- Only two QA configurations were chosen: can they represent all? (A counter example: ITER tokamak is also a special case of QA.)
- A systematic theory is required: which factors cause the different transport level? How can we reduce the transport level in QA?

This talk: characterizing the transport properties of quasisymmetric stellarators from their equivalent tokamaks

Quasisymmetry (QS): $|\boldsymbol{B}| = B(\psi, M\vartheta - N\zeta)$ in Boozer coordinates. They share many more similar properties with tokamaks.

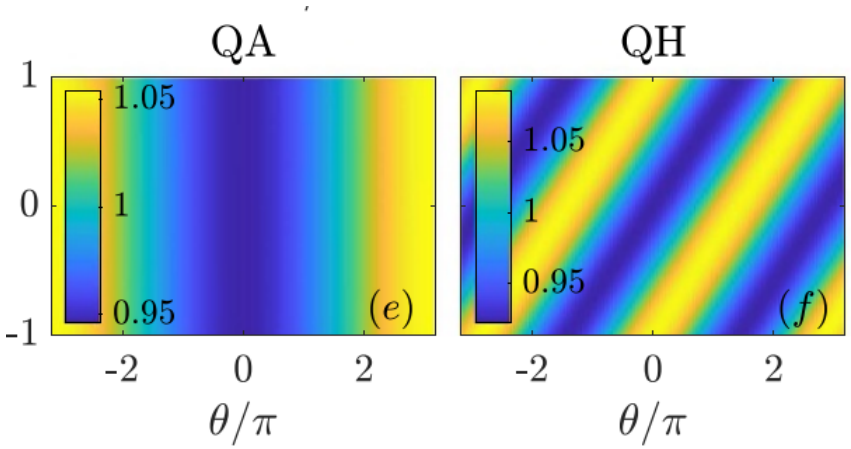

For different QA and QH stellarators, we wish to first convert them to "equivalent tokamaks", and then make fair comparisons:

1. Theoretical background: local gyrokinetic formulation.
2. Derivation of equivalent tokamaks from near-axis expansion.
3. 1st-order results: circular tokamaks and their transport levels.
4. 2nd-order results and local Miller equilibria.

1. Theoretical background: local gyrokinetic formulation

Local gyrokinetic simulations study a thin "flux tube" along $\boldsymbol{B} = \nabla\psi \times \nabla\alpha$:[1]

- $\psi \approx B_0 r^2/2$: toroidal magnetic flux over 2π.
- $\alpha = \vartheta - \iota\zeta$: field-line label.
- Define $\nabla x = \nabla\psi/B_0 r, \nabla y = r\nabla\alpha$.
- WKB approximation: $\nabla \to i\boldsymbol{k}/\rho_* + \nabla_\parallel$, with $\boldsymbol{k} = k_x \nabla x + k_y \nabla y$ and $\rho_* = \rho_i/a \ll 1$.

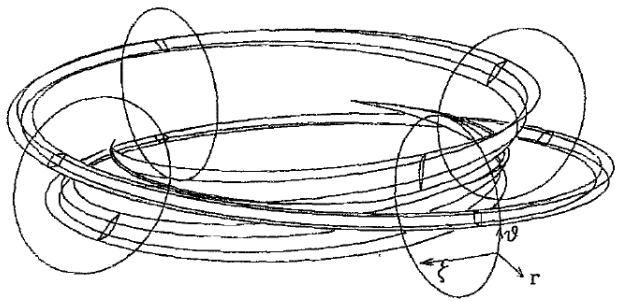

Electrostatic (linear) gyrokinetic equation:

$$\frac{\partial h}{\partial t} + v_\parallel k_\vartheta \frac{\partial h}{\partial \vartheta} + \boldsymbol{v}_D \cdot \nabla h = \frac{Ze}{T}\frac{\partial \langle\Phi\rangle}{\partial t} + \left[\kappa_n - \kappa_T\left(\mathcal{E} - \frac{3}{2}\right)\right]\frac{1}{2}\frac{\partial \langle\Phi\rangle}{\partial y}.$$

$h = h(x, y, \vartheta, \mathcal{E}, \lambda)$ is the nonadiabatic part of the distribution function, $\langle\Phi\rangle$ is the gyroaveraged potential, $\kappa_n = a/L_n$ and $\kappa_T = a/L_T$.

[1] M. Beer, S. Cowley, and G. Hammett, Phys. Plasmas **2**, 2687 (1995).

Electrostatic local simulations involve 8 functions (1D functions along field lines)

- Normalized magnetic field $B_N = B/B_a$ (bmag).
- The (inverse) parallel connection length $k_\vartheta = (\partial l/\partial\vartheta)^{-1}$ (gradpar).

$$\hat{\boldsymbol{b}} \cdot \nabla\vartheta = \text{gradpar} \cdot \partial_\vartheta .$$

- The magnetic-drift term $\boldsymbol{v}_D \cdot \nabla h = i(T/Ze)\omega_D h$ with the drift frequency:

$$\omega_D = \frac{k_y}{2}\left[\frac{v_\perp^2}{2}\left(\text{gbdrift} + \text{gbdrift0}\cdot\frac{k_x}{k_y\hat{s}}\right) + v_\parallel^2\left(\text{cvdrift} + \text{cvdrift0}\cdot\frac{k_x}{k_y\hat{s}}\right)\right].$$

$$\text{gbdrfit} \propto \boldsymbol{B}\times\nabla B\cdot\nabla y, \quad \text{cvdrfit} \propto \boldsymbol{B}\times\boldsymbol{\kappa}\cdot\nabla y$$

$$\text{gbdrift0} = \text{cvdrift0} \propto \hat{s}\boldsymbol{B}\times\nabla B\cdot\nabla x.$$

$\boldsymbol{\kappa} = \hat{\boldsymbol{b}}\cdot\nabla\hat{\boldsymbol{b}}$: curvature, $\hat{s} = (r/q)(dq/dr)$: magnetic shear.

- The perpendicular wavenumber from gyroaverage $\langle\Phi\rangle = J_0(k_\perp\rho_i)\Phi$:

$$k_\perp^2(\vartheta) = |k_x\nabla x + k_y\nabla_y|^2 = k_y^2\left|\text{gds2} + 2\frac{k_x}{k_y\hat{s}}\text{gds21} + \left(\frac{k_x}{k_y\hat{s}}\right)^2\text{gds22}\right|,$$

with $\text{gds2} = |\nabla y|^2, \text{gds21} = \hat{s}\nabla x\cdot\nabla y, \text{gds22} = \hat{s}^2|\nabla x|^2$.

- 8 different functions since gbdrift0=cvdrift0.

QS configurations look very similar to tokamaks from local gyrokinetic simulations

For QS stellarators, different field lines share more similiarties than differences:[1]

- Five field-line-independent functions: bmag, gradpar, gbdrift, cvdrift, gbdrift0=cvdrift0.
- Three field-line-dependent functions: gds2, gds21, gds22.

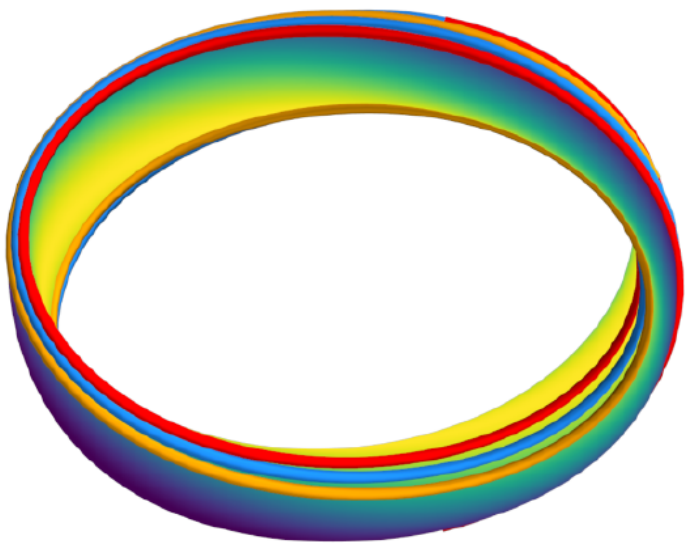

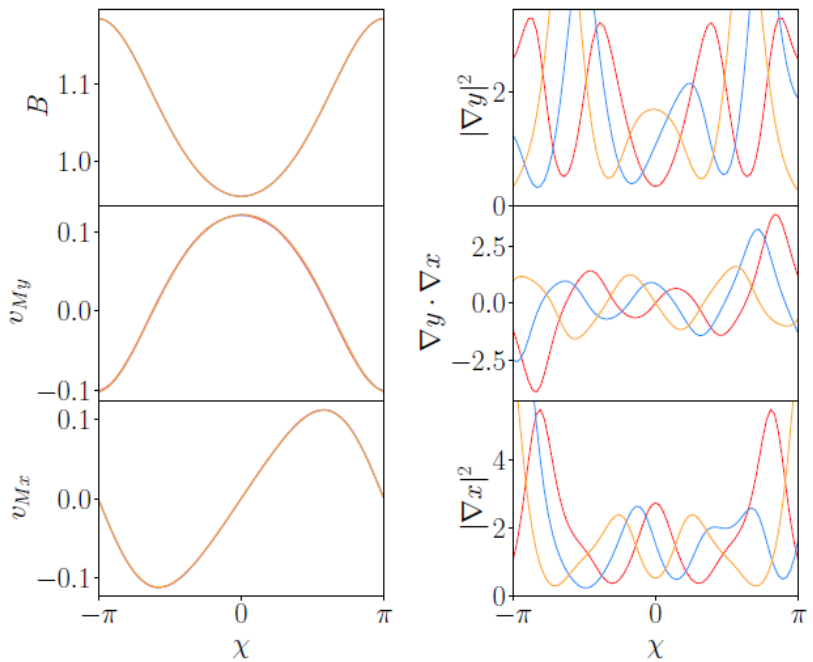

[1] R. Nies, Ph.D. thesis proposal, Princeton University.

Equivalent tokamak: a tokamak with the same bmag, gradpar, gbdrift, cvdrift, and cvdrift0 as the QS stellarator

For a stellarator configuration, we can calculate these quantities along field lines.

Can we find a tokamak equilibrium, with the same geometric quantities?

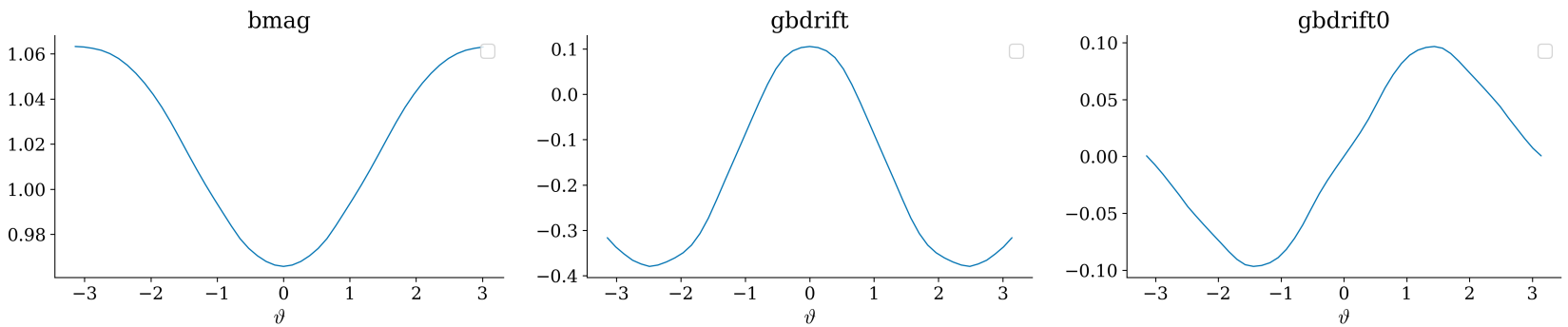

Figure 4: Geometric quantities for the QA configuration studied by Chen *et al.*.

2. Derive equivalent tokamaks from the near-axis expansion (NAE) theory

- Magnetic fields in Boozer coordinate (ψ, ϑ, ζ):

$$\boldsymbol{B} = G(\psi)\nabla\zeta + I(\psi)\nabla\vartheta + \delta(\psi,\vartheta,\zeta)\nabla\psi.$$

- Expand quantities in terms of $r = \sqrt{2\psi/B_0}$:[1]

$$G = G_0 + G_2 r^2 + \ldots, \quad I = I_2 r^2 + \ldots, \quad p = p_0 + p_2 r^2 + \ldots$$

$$B = B_0 + B_1 r + B_2 r^2 + \ldots, \quad \delta = r\delta_{1s}\sin\vartheta + \ldots$$

- 1st order in r: variation of B in ϑ determined by a free parameter $\bar{\eta}$

$$B \approx B_0(1 - \bar{\eta} r\cos\vartheta)$$

  The rotational transform ι_0 is determined by $\bar{\eta}$ and I_2.

- 2nd order: MHD force balance $G_2 = \iota_0 I_2 - \mu_0 p_2 G_0/B_0^2$, $\delta_{1s} = -4\mu_0 p_2 G_0 \bar{\eta}/\iota_0 B_0^3$, triangularity, Shafranov shift, etc.
- 3rd order: higher-order shaping and magnetic shear, but generally no solution as the system becomes overdetermined.[2]

[1] M. Landreman and W. Sengupta, J. Plasma Phys. **85**, 815850601 (2019).
[2] D. Garren and A. Boozer, Phys. Fluids B 3, **10** (1991).

Calculation of geometric quantities from the NAE

- Geometric quantities with 1st-order accuracy:

$$\text{bmag} = \frac{B}{B_0} \approx 1 - \bar{\eta} r \cos\vartheta.$$

$$\text{gradpar} \approx \frac{\iota a B_0}{G(0)} = \frac{\iota a}{R}, \quad R = \frac{G(0)}{B_0}$$

$$\text{cvdrift0} = \text{gbdrift0} = 2\bar{\eta} a \hat{s} \sin\vartheta$$

$$\text{cvdrift} = 2\bar{\eta} a \left[\cos\vartheta + \left(\hat{s}\vartheta + \epsilon^2 \beta' \sin\vartheta\right) \sin\vartheta\right]$$

$$\text{gbdrift} = \text{cvdrift} + \beta',$$

  where $\epsilon = \bar{\eta} r$, $\beta' = 4\mu_0 p_2 a r / B_0^2$, $\hat{s}$ is the magnetic shear.

- Tokamak (a special case of the QA) can also be described from the NAE:

$$\text{bmag} \approx 1 - \frac{r}{R}\cos\vartheta, \quad \text{gradpar} = \frac{\iota a}{R}, \quad \text{cvdrift0} = 2\frac{a}{R}\hat{s}\sin\vartheta, \quad \ldots$$

  ($\bar{\eta} = 1/R$ for circular tokamaks).

3. 1st-order theory: equivalent tokamaks with circular flux surfaces

To the 1st order, we can find equivalent tokamaks for QA stellarators with circular flux surfaces, with the same minor radius a: .

- Match cvdrift=gbdrift and cvdrift0=gbdrift0: $R^t = 1/\bar{\eta}$.
- Match of gradpar: $\iota^t = \iota^s/\bar{\eta}R^s$, $R^s = G(0)/B_0$.
- Match the secular behavior in cvdrift: $\hat{s}^t = \hat{s}^s$.
- Match bmag: $r^t = r^s$.
- Match the difference between cvdrift and gbdrift: $p_2^t = p_2^s$.

Geometrically, the equivalent tokamaks are characterized by 3 factors:

- aspect ratio R/a; rotational transform ι; magnetic shear $\hat{s}$
- Note that the equivalent tokamak does not need be circular: it happens to be circular because we assumed the same a.

For QH configurations, they are isomorphic to QA configurations with the following transform:

- $\theta^{\text{new}} = (1 - \iota N)\theta^{\text{old}}, \quad \iota^{\text{new}} = \iota^{\text{old}} - N, \quad \hat{s}^{\text{new}} = \hat{s}^{\text{old}}\iota^{\text{old}}/\iota^{\text{new}}$.
- Correspondingly, gradpar$^{\text{new}}$=gradpar$^{\text{old}}\iota^{\text{new}}/\iota^{\text{old}}$.

Examples: the Landreman-Buller-Drevlak QS configurations studied by Chen *et al.*

- Straight pressure profile: $p \approx p_0(1-s)$, $p_0 = 7 \times 10^5$Pa. Reactor scale $B_0 = 5.7$ T and $a = 1.7$ m.
- QA: $R = L_{\text{axis}}/2\pi = 10.7\text{m}$, $\iota = 0.4$, $\hat{s} = -0.45$ at mid radius, and $\bar{\eta} \approx 0.055\text{m}^{-1}$, $N = 0$.
- QH: $R = L_{\text{axis}}/2\pi = 13.9\text{m}$, $\iota = 1.1$, $\hat{s} = 0.07$ at mid radius, and $\bar{\eta} \approx 0.128\text{m}^{-1}$, $N = 4$.

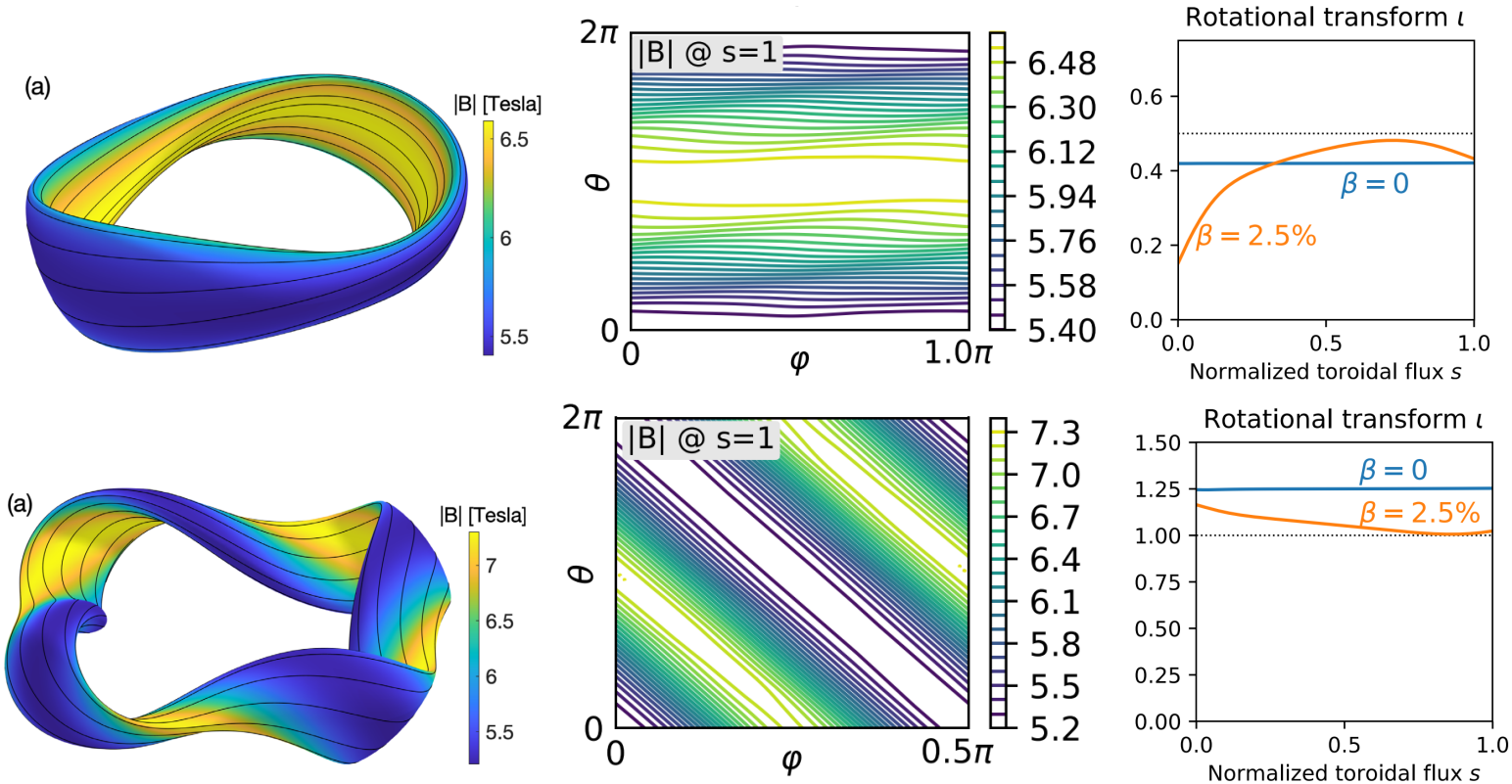

Equivalent tokamaks for the the Landreman-Buller-Drevlak QS configurations

With the same $a = 1.7$m and $B_0 = 5.7$T, the equivalent tokamaks are:

- for the QA: $R/a = 10.7$, $\iota = 0.63$, $\hat{s} = -0.45$.
- for the QH: $R/a = 4.6$, $\iota = 1.7$, $\hat{s} \approx 0$.

Major differences:

- Large R/a for QA due to smaller $\bar{\eta}$ (QH is much more compact).
- Large ι for QH due to the transformation $\iota \to |\iota - N|$ with $N = 4$.

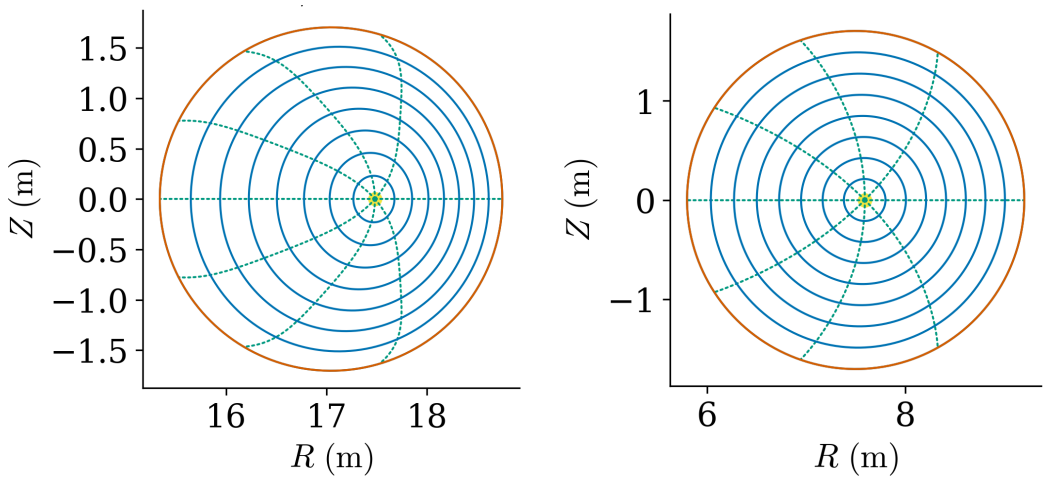

Figure 5: Flux surfaces of equivalent tokamak of the QA (left) and QH (right). These are global MHD equilibria solved from DESC.

[1] https://desc-docs.readthedocs.io/

Comparison of transport level between QS and their equivalent tokamaks from global GTC simulations

Simulation setup similar to the above mentioned paper (gyrokinetic ions, adiabatic electrons, etc.), with a higher temperature gradient.

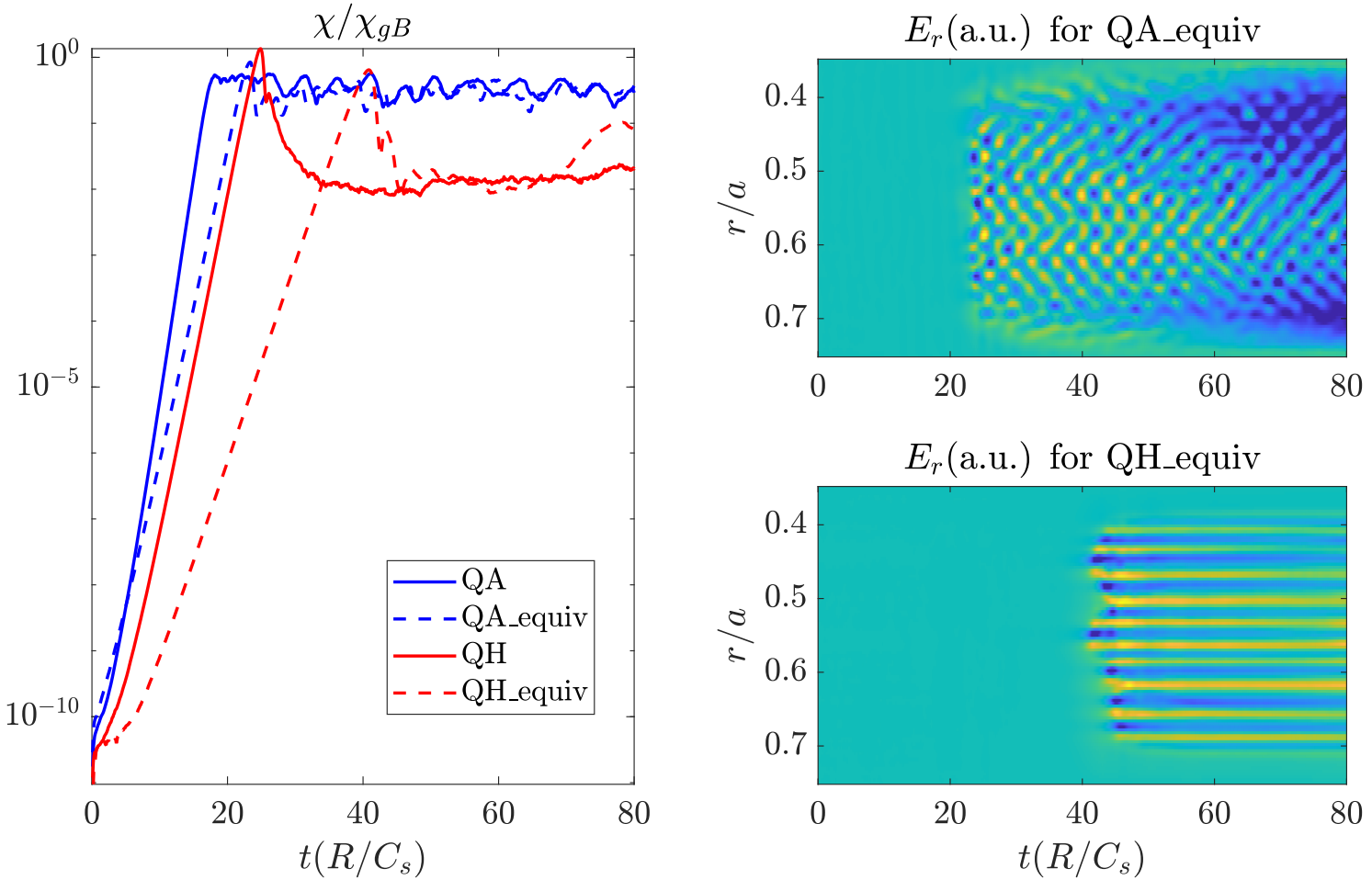

Figure 6: Left: the heat diffusivity $\chi = Q/n|\nabla T|$ in gyro-Bohm unit $\chi_{gB} = \rho_s^2 C_s/L_T$. Right: the zonal radial electric field (arbitrary unit) versus radius r/a and time t.

4. More accurate theory: 2nd-order NAE

The above 1st-order theory is not accurate enough. Magnetic-field strength up to 2nd order:

$$B = B_0 + B_{1c} r \cos\vartheta + [B_{20} + B_{2c}\cos(2\vartheta)] r^2, \quad B_{1c} = -\bar{\eta}.$$

$$\frac{dB}{dr} = B_{1c} + 2r[B_{20} + B_{2c}\cos(2\vartheta)], \quad \text{gbdrift} \propto -\frac{1}{B}\frac{dB}{dr}.$$

Even though the QA and the tokamak share the same B_{1c}, they still have different B_{20} and B_{2c}, so the error is actually 1st order in r.

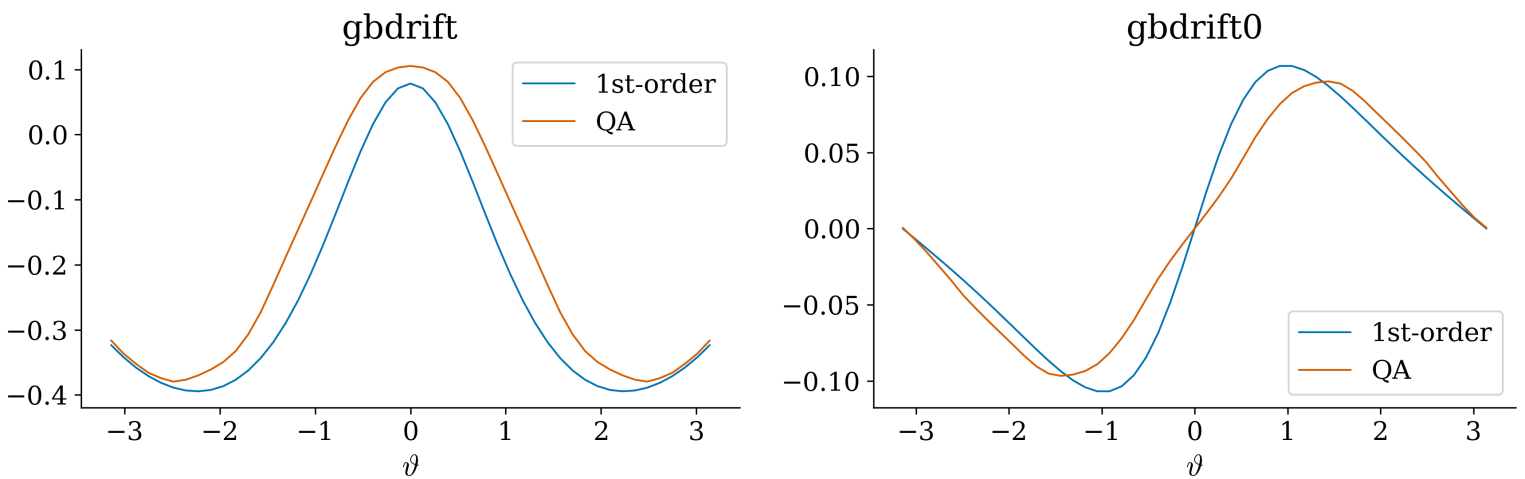

Figure 7: Comparison of gbdrift and gbdrift0 between the QA and the circular tokamak at $r/a = 0.5$.

Calculate B_{20} for tokamaks from the NAE theory

Landreman and Sengupta (JPP 2019) provided a systematic procedure to calculate coefficients from the NAE. The free parameters are:

- 1st order: $\boldsymbol{R}_{\text{axis}}$, $\bar{\eta}$, and I_2 (hence ι).
- 2nd order: p_2, B_{2c}.
- All other quantities can be calculated based on these parameters.

Things are greatly simplified for tokamaks with axisymmetry, obtaining (assuming $R_0 = B_0 = 1$)

$$B_{20}^t(\bar{\eta}, I_2, p_2, B_{2c}) = -3\,\frac{\bar{\eta}^4 - 1}{\bar{\eta}^4 - 3}\,B_{2c} + \mu_0 p_2\,\frac{(\bar{\eta}^4+1)^2 - 2I_2^2(\bar{\eta}^4 - 3)}{2I_2^2(\bar{\eta}^4 - 3)} + \frac{\bar{\eta}^2\left(2\bar{\eta}^{12} - 3\bar{\eta}^8 - 12\bar{\eta}^4 - 7 + 8I_2^2\bar{\eta}^4(2 - \bar{\eta}^4)\right)}{2(\bar{\eta}^4 - 3)(\bar{\eta}^4+1)^2}$$

Construct equivalent tokamaks with 2nd-order accuracy?

With 1st-order and 2nd-order quantities given, the equivalent tokamak is 2nd-order accurate if and only if $B_{20}^t = B_{20}^s$.

Not all QS stellarator have equivalent tokamaks with the same B_{20}, as the system becomes overdetermined.

- But solutions do exist for some stellarators.
- For example, for the Landrenman-Buller-Drevlak QA configuration, a good approximate solution could be found.
- For the Landrenman-Buller-Drevlak QH configuration, we can still find an approximated equivalent tokamak, but the agreement is not as good.

Examples of the 2nd-order equivalent tokamaks for the QA

The agreement between the QA and the equivalent tokamaks is improved with the introduction of 2nd-order quantities (elongation, triangularity, Shafranov shift etc.)

- A good fit was found for the QA: $R/a = 10.2$, $\iota = 0.65$, $\hat{s} = -0.45$, $\kappa = 1.67$, $\Delta \approx 0$, $\partial_r R_0 = 0.15$.
- An okay fit was found for the QH: $R/a = 5.1$, $\iota = 1.63$, $\hat{s} \approx 0$, $\kappa = 0.87$, $\Delta = -0.22$, $\partial_r R_0 = 0.17$.

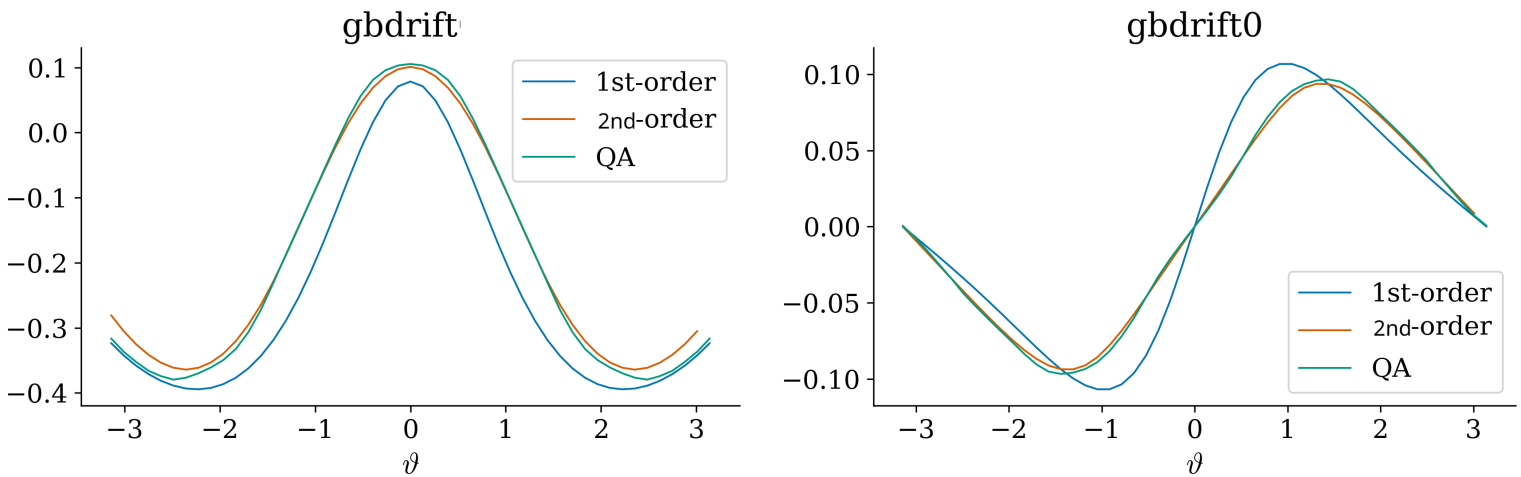

Figure 8: Comparison of gbdrift and gbdrift0 between the QA, circular tokamak, and the 2nd-order equivalent tokamak parameterized by a local Miller equilibrium (Miller *et al.* Phys. Plasmas **5**, 973 (1998)).

Transport properties remain similar with 2nd-order equivalent tokamaks

Since the 2nd-order equivalent tokamaks are modeled with local Miller equilibria, the simulations done here are from a local gyrokinetic code GX.[1]

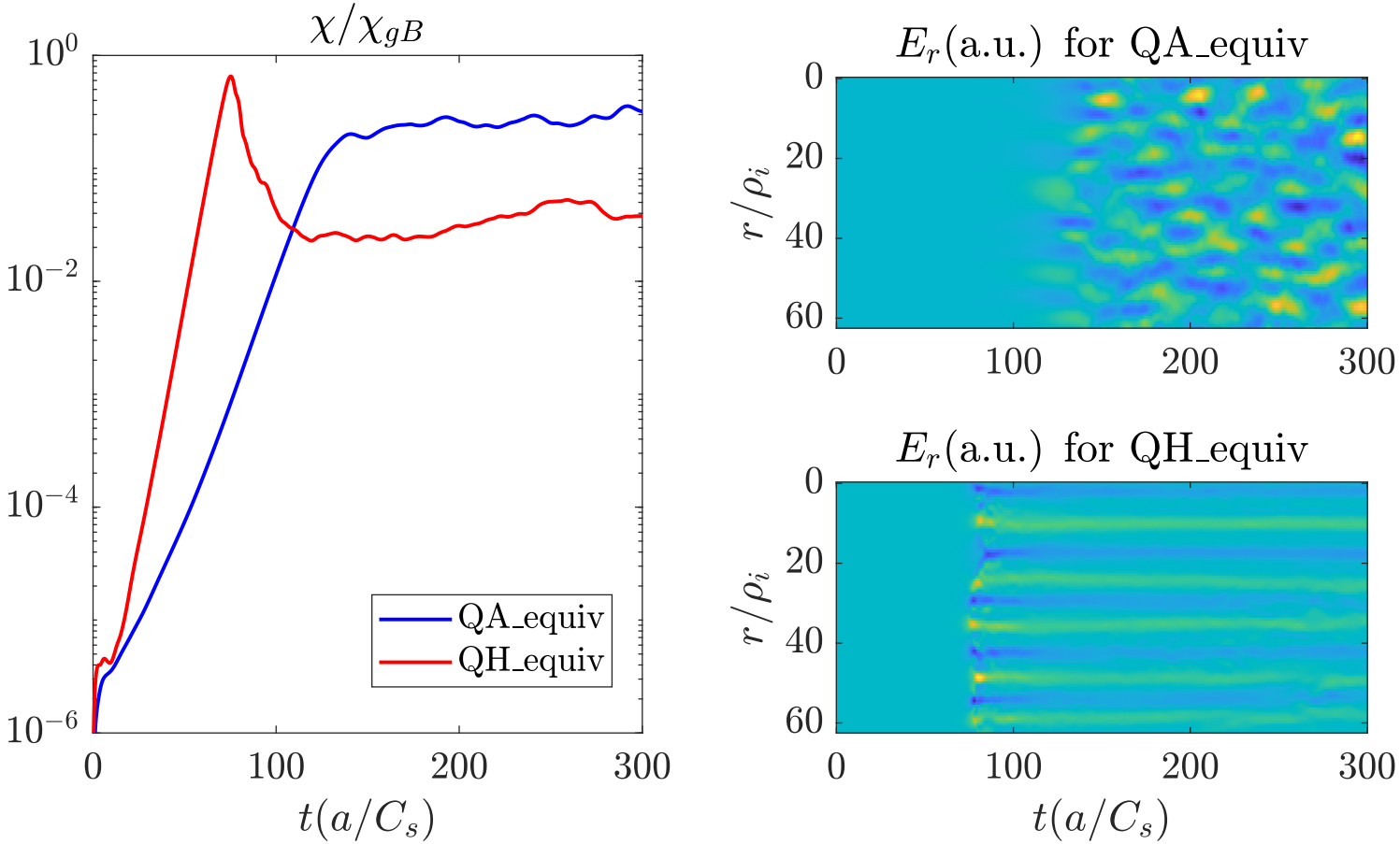

Figure 9: Left: the heat diffusivity $\chi = Q/n|\nabla T|$ in gyro-Bohm unit $\chi_{gB} = \rho_s^2 C_s/L_T$. Right: the zonal radial electric field (arbitrary unit) versus radius r/ρ_i and time t.

[1] https://gx.readthedocs.io/en/latest/

Conclusions: key differences between the QA and QH in terms of their equivalent tokamaks

Compare the equivalent tokamaks of the QA and the QH:

- The QH is much more compact, $R/a \approx 5$, due to its larger $\bar{\eta}$ parameters.
- The QH has a much larger ι, due to the coordinate transform resulting $\iota \to |\iota - N|$,$N = 4$.
- Both factors seem to contribute to the lower transport level in the QH compared to the QA.

Questions remain:

- Effects from the magnetic shear: for the configurations studied here, QA has $\hat{s} < 0$; but QH has $\hat{s} \approx 0$, again due to the coordinate transform resulting $\iota \to |\iota - N|$. Is it a general behavior?
- Still need a systematic nonlinear turbulence theory. Which better also includes QI.